J. Sci. Soc. Thailand 13 (1987) 85-106

APPLICATION OF BOUNDARY INTEGRAL EQUATIONS TO THE PENETRATION PROBLEM

SUDHIRA WASUWANICH

Department of Mathematics, Faculty of Science, Kasetsart University, Bangkok 10900, Thailand

(Received 27 April 1987)

Abstract

The present paper is a study of the formation of chips due to the penetration of a rigid wedge into brittle-elastic material such as rock.

The analysis of stress field has been numerically calculated by using published Boundary Integral Equations. It is found that the position of crack initiation is along the normal line from middle upper part of the wedge to the wedge side. When the load is increased less than 1.24 % beyond the critical limit fracture begin to propagate. Consequently the interior damaged region is growing around the wedge. The growing damaged region becomes more shallow and longer in the direction parallel to the wedge side. It grows in both horizontal and vertical directions. Stress near the damaged region is much more affected than stress far away. The stress path at some point is changed from the straight line to a curve with upward concavity. If the load is increased more than 1.24% of critical load the fracture becomes unstable.

Introduction

Methods of analysis in most scientific and engineering fields including modern technology have been revolutionized by the advent of the modern digital computer. Now that various procedures have been developed by analysts working at all levels from fairly pure research to quite specific applications, the Boundary Integral Element (B.I.E.) technique has evolved to a high level of performance and its usefulness has also been broadly accepted in a wide range of situations.

The B.I.E. methods, having their origins in classical elasticity, have only in recent years begun to play a significant role in solid mechanics[1,2]. Solutions to problems in elasticity and elasto-plasticity by B.I.E. methods have been obtained by many workers[3,4,5]. The extension of the B.I.E method to fracture mechanics has received much less attention. The basic theories and equations have been formulated[6], but few applications have been reported. The purposes of this paper are to review one of these applications and present details of the analysis as applied to the penetration problem.

Background

The two-dimensional isotropic elastic-brittle solid (rock) due to the penetration of a rigid wedge is shown in Figure 1, namely a two-dimensional wedge-shaped indentor.

The wedge force 2F is applied to the rock mass. As the wedge force F is increased to the critical limit, some cracks are observed. If the force is increased beyond the critical limit, these cracks begin to propagate in a slow stable manner in the sense that, if loading is stopped and the stress level is maintained at a certain value, crack propagation ceases. If the force is further increased the crack system is developed to such a stage that it becomes unstable and the release of stain energy is sufficient to make the cracks self-propagating until complete disruption and failure occurs. Consequently, a resulting chip is removed from the rock mass.

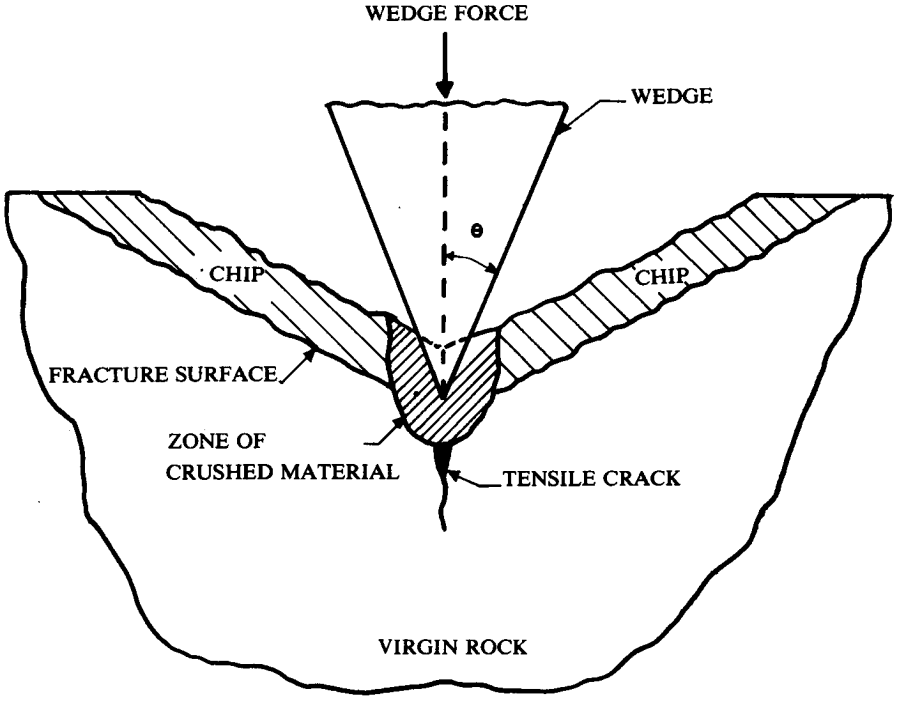

Figure 1 The penetration of a rigid wedge-shaped indentor to the rock mass.

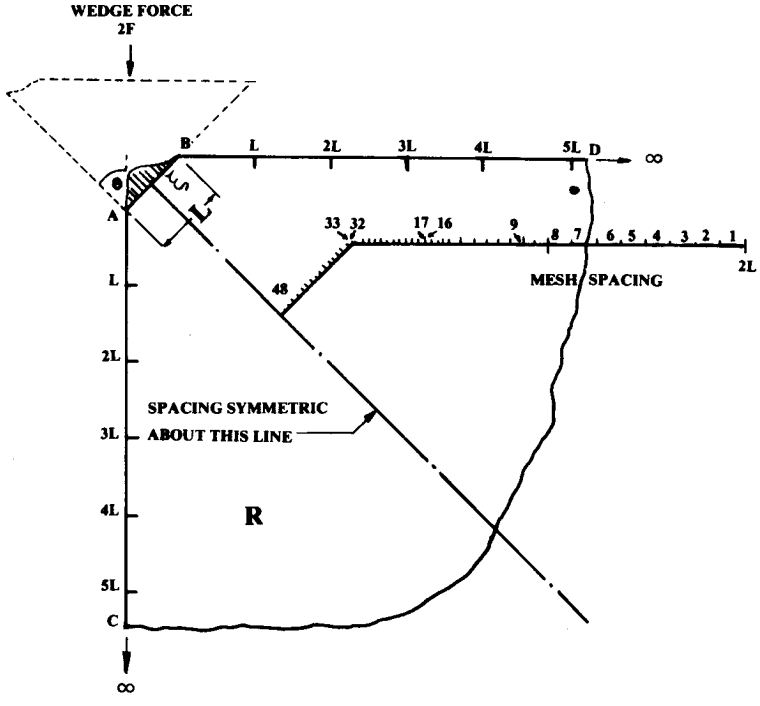

Figure 2 The distribution of wedge-force 2F along the edge AB of a quarter plane R. The boundary ABDC is divided to 96 elements.

The major difficulty is to describe the chipping phase mathematically, i.e. the force at which the chip is formed, the chip geometry etc. This involves many major assumptions. For the sake of simplicity, this penetration problem has been formulated by considering a truncated quarter plane R with specified traction on the boundary as shown in Figure 2. Sikarski and Alterio[7] solved this problem by assuming linear elastic material behavior. They used the B.I.E to obtain the stress distribution in the quarter plane region R and proposed a fracture path based on the assumption that the stress distributions are unaffected by the propagating crack. Clearly, when the traction is increased to the critical limit, i.e. at some points the material behaves inelastically, fracture will initiate at surrounding points forming a growing region of damage and this will affect the original stress field. Consequently, the fracture path will be preliminary and this should be modified, so that it is necessary to adjust the stress field accordingly.

In this presentation, a method of analysis developed in ref. 8 is applied to this particular problem. An attempt is made to adjust the stress field to take account of the

effect of the damage region growth by considering it as a pseudo-body force. By using numerical calculation, it is possible to determine

(1) the load and the point of initiation

(2) the shape of the damaged region.

Analysis

The boundary value problem to be analyzed, namely the formation of chips in a two-dimensional (plane stress) isotropic elastic-brittle solid (rock) due to the penetration of a rigid wedge, is shown in Figure 2. The specified tractions on the boundary are given by

$$t_n = \begin{cases} 0 & \text{on BD} \\ p\,(\xi/L)^m\,(1 - \cos 2\pi\xi/L) & \text{on AB} \\ 0 & \text{on AC} \end{cases} \qquad \text{.....(1)}$$

$$t_s = 0 \quad ,$$

where t_n, t_s are the normal and tangential traction components, ξ is a coordinate on AB of legnth L defined in Figure 2, m is a form of parameter, the higher value of which means the more asymmetric and concentrated traction distribution, p is a scalar pressure which can be related to the half wedge force F as follows,

$$p = \frac{F \cos \phi_f}{L \sin(\theta + \phi_f) \int_0^1 \eta^m (1 - \cos 2\pi\eta)\, d\eta} \quad , \qquad \text{.....(2)}$$

where θ is the half wedge angle and ϕ_f is the friction angle. For p defined by equation (2), all tractions are added up to the same value of F/L (the vertical force component).

Note the given traction is pertinent to the wedge penetration problem i.e., the tangential traction component is due to friction between the wedge and material.

To perform the analysis, the following basic tools are required:

1. stress field determinations which must be calculated before cracks are observed and after they are incipient.

2. a fracture criterion based on Mohr's criterion which will define the boundary between an elastic and an inelastic region.

Stress Field for the Region with No Damage in Two-Dimensions.

The stress field solutions in linear elasticity by both direct formulation[3,4,6] and indirect formulation[5,8,9] have been discussed in detail. A brief discussion following Alterio and Sikarski[10] in the indirect method will be reviewed.

The region of interest is embedded in an infinite (fictitious) plane of the same material for which the Green's function $\Sigma_{ij}^{(q)}(Q, P)$ and $U_i^{(q)}(Q, P)$ are known. $\Sigma_{ij}^{(q)}(Q, P)$ represents the ijth stress component at a field point $Q(\xi_1, \xi_2)$ due to a unit point force in the q direction at the boundary point $P(x_1, x_2)$ in the region. $U_i^{(q)}(Q, P)$ represent the displacements at a field point Q in the ith direction due to a unit point force at P on the boundary in the q direction. $U_i^{(q)}(Q, P)$ and $\Sigma_{ij}^{(q)}(Q, P)$ can be expressed as:

$$U_i^{(k)} = \frac{1}{8\pi\,\mu(1-\nu)} \left[(3-4\nu)\,\ln\frac{1}{r}\,\delta_{ik} + \frac{r_i\,r_k}{r^2}\right],$$

$$\Sigma_{ij}^{(k)} = -\frac{1}{4\,\pi(1-\nu)}\,\frac{1}{r}\left[\frac{r_i}{r}\,\delta_{jk} + \frac{r_j}{r}\,\delta_{ki} - \frac{r_k}{r}\,\delta_{ij}\,(1-2\nu) + 2\,\frac{r_i r_j r_k}{r^2}\right],$$

where $r = [(x_1 - \xi_1)^2 + (x_2 - \xi_2)^2]^{1/2}$

A fictitious traction $\vec{p}^{\,*}$ (unknown) now acts along the boundary ABDC, and the stress and displacement component due to $\vec{p}^{\,*}$ are

$$\sigma_{ij}(Q) = \int_{ABDC} \Sigma_{ij}^{(q)}(Q,P)\; p_q^*(P)\; ds(P) \qquad \text{.....(3)}$$

$$u_i(Q) = \int_{ABDC} U_i^{(q)}(Q,P)\; p_q^*(P)\; ds(P) \qquad \text{.....(4)}$$

where P is on the boundary ABDC and ds is an element of the length along the boundary ABDC. This must satisfy the boundary conditions

$$\sigma_{ij} n_j = t_i \qquad \text{on ABDC} \qquad \text{.....(5)}$$

where n_j is the direction cosine of the normal at a point on the boundary ABDC and t_i is the specified traction component.

To find the unknown fictitious traction vector $\vec{p}^*$, let Q tend to point P′ on the boundary ABDC and substitute (5) into (3) and extract the singularity when P′ coincides with P in the Cauchy Principal Value sense. This leads to

$$\frac{1}{2} p_i^*(P') + \int_{\substack{ABDC \\ P' \neq P}} \Sigma_{ij}^{(q)}(P',P) p_q^*(P) n_j(P') ds(P) = t_i(P') \quad \text{.....(6)}$$

Once the fictitious traction vector $\vec{p}^*$ is determined (by numerical calculation) the stresses anywhere in the field are founded by substituting $\vec{p}^*$ into equation (3). This is important feature since it will be necessary to search the field for the point of fracture initiation.

Initiation of Damage and Initial Damaged Zone.

In order to find the load that causes the macrofracture at some point in the material, it is necessary to postulate the fracture criterion which will define the onset of brittle condition. This is analogous to the yield condition of plasticity. Vile[11] found that the fracture envelopes for both the initial and final failure for aggregate concrete, similar to rock, are very similar in shape. They exhibit very rounded envelopes so it is reasonable to use the Mohr's criterion as the fracture criterion.

Based on the condition for tangency of Mohr's criterion and Mohr's circle for the state of principal stresses $\bar{\sigma}_1$, $\bar{\sigma}_2$, it can be shown by using the argument discussed by Alterio[12] that the elastic surface (see Figure 3) is given by,

$$f_F(\bar{\sigma}) = 0 \quad , \qquad \text{.....(7)}$$

where

$$f_F(\bar{\sigma}) = (\bar{\sigma}_1 - \bar{\sigma}_2)^2 - (m_i - 1) S_t \, \beta(\bar{\sigma}, m_i) \quad \text{if } m_i(m_i - 2)\bar{\sigma}_1 + \bar{\sigma}_2 < 0$$

$$= \bar{\sigma}_1 - S_t \quad \text{if } m_i(m_i - 2)\bar{\sigma}_1 + \bar{\sigma}_2 \geq 0 \, , \qquad \text{.....(8)}$$

and

$$\beta(\bar{\sigma}, m_i) = 2\left[\sqrt{(\bar{\sigma}_1 - \bar{\sigma}_2)^2 + (m_i - 1)^2 \bar{\sigma}_1 \bar{\sigma}_2} - (m_i - 1)(\bar{\sigma}_1 + \bar{\sigma}_2)\right] ,$$

$$m_i = \sqrt{(S_c^i / S_t)}$$

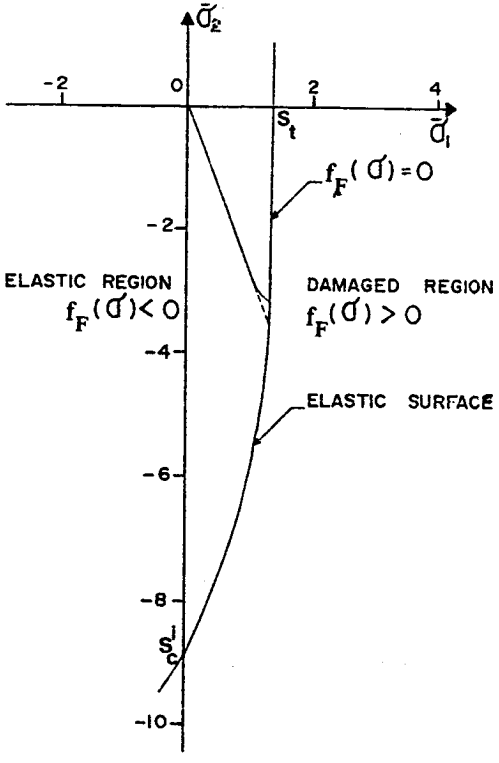

Figure 3 Elastic surface following equations (7) and (8). The stress path of the point at the position number 93 is concave upward after the stress has been corrected.

Here S_c^i is the uniaxial compressive stress magnitude at which microcrack growth was first observed where as S_t is the tensile strength of the material. If the stress state at any point is inside or on the elastic surface i.e., $f_F(\bar{\sigma}) \leq 0$, this means that the behavior of the material at that point remains elastic. If the point that lies outside the elastic surface i.e., $f_F(\bar{\sigma}) > 0$, it means that there is the possibility of crack initiation and the behavior of material at that point is no longer elastic. Nondimensionalized $\bar{\sigma}_1$, $\bar{\sigma}_2$ by $\sigma_1 = \bar{\sigma}_1/(F/L)$, $\sigma_2 = \bar{\sigma}_2/(F/L)$ gives the Fracture function $K^i(\sigma, S_t, S_c^i)$ defined by

$$K^i(\sigma, S_t, S_c^i) = F/L = \frac{S_t(m_i - 1)}{(\sigma_1 - \sigma_2)^2}\,\beta(\sigma, m_i) \quad \text{if } m_i(m_i - 2)\sigma_1 + \sigma_2 < 0 \qquad \text{.....(9)}$$

$$= S_t/\sigma_1 \quad \text{if } m_i(m_i - 2)\,\sigma_1 + \sigma_2 \geq 0$$

The fracture function $K^i(\sigma, S_t, S_c^i)$ defined in this manner can be interpreted physically[12] as the value of loading F/L necessary to initiate grain damage at a location in the field at which the stress state is σ_1, σ_2. The contour plot of K^i can be constructed. Each contour represents the global force level F/L necessary to propagate the region of damage to that contour. These contours are preliminary and have to be corrected since we assumed that the growing region of damage does not affect the elastic field outside of the region. The crack will be initiated at the point where K^i is minimum. If the load F/L is increased by Δ F/L beyond the minimum of K^i, fracture will be initiated and propagate at points in the vicinity of the point where K^i is minimum and a growing region of damage is formed.

Constitutive Equations

In order to find the growing damaged region, it is necessary to define fracture parameter ϕ_{ij} known as "crack tensor" which will characterize the intensity and geometry of crack field in a body of consideration. Dragon[13] postulated that the opening of the crack occurs in some particular principal direction of stress. Thus, the development of fracturing is related to the increments of the positive stress deviator components. However, there are stress paths for which no cracks appear and consequently no increments in any components of the crack tensor. In modelling the development of crack tensor, the kinetics of brittle fracture should be taken into account. This will provide relations connecting increments of ϕ_{ij} and stress or strain increments. Dragon[13,14] assumed that the kinetics of brittle fracture proceed if the actual state of stress satisfies inequalities

$$f_F(\sigma) \geq 0 \qquad \text{.....(10)}$$

where $f_F(\sigma)$ is given by equation (8). Geometrically speaking, $f_F(\sigma)$ represents an elastic surface which separates a purely elastic state from a state of progressive fracture.

Let the principal components of the crack (ϕ_i) and the principal stress deviator (s_i) be as given in ref. 13:

$$\begin{aligned} d\phi_i &= g_F(\sigma) ds_1 \quad \text{if} \quad f_F(\sigma) \geq 0 \quad \text{for all i such that} \\ &\qquad s_i \geq 0 \ \text{and} \ ds_i \geq 0 \\ &= 0 \quad \text{for remaining i,} \\ d\phi_i &= 0 \quad \text{if} \quad f_F(\sigma) < 0 \qquad \text{in any case.} \end{aligned} \qquad \text{.....(11)}$$

The coefficient $g_F(\sigma)$ is a positive real valued function obtained from $f_F(\sigma)$. The $g_F(\sigma)$ involves the influence of actual stresses on fracturing and on particular stress path. One can find the crack tensor in general coordinate by using the orthogonal transformation defined by θ_{mn} so we obtain any arbitrary component

$$d\phi_{ij} = \sum_{n=1}^{2} \theta_{in}\, \theta_{jn}\, d\phi_n$$

To obtain ϕ_i one can integrate $d\phi_i$ along the stress path and using the orthogonal transformation to obtain ϕ_{ij}.

By assuming the existence of an elastic potential function and the kinetics of the brittle fracture which satisfies inequalities (10) following Dragon[13], one can show that the fracturing strain increment $d\epsilon_{ij}^{(f)}$ can be written as

$$d\epsilon_{ij}^{(f)} = \frac{B(\phi)}{2G_s^2\,(\phi_{rs})}\,\sigma_{ij}\,(\phi_{kk}\delta_{mn} + \phi_{mn})d\phi_{mn} \qquad \text{for } i \neq j \qquad \text{.....(12)}$$

$$d\epsilon_{jj}^{(f)} = \left[\sigma_{jj}\frac{B(\phi)}{2G_s^2\,(\phi_{rs})} - \sigma_{kk}\,\frac{(A(\phi)}{9K_s^2\,(\phi_{rs})} + \frac{B(\phi)}{6G_s^2\,(\phi_{rs})}\right](\phi_{kk}\delta_{mn} + \phi_{mn})d\phi_{mn}$$

$$\text{for } i = j \qquad \text{.....(13)}$$

and volumetric parts

$$d\ell_{jj}^{(f)} = -\sigma_{kk}\,\frac{A(\phi)}{3K_s^2\,(\phi_{rs})}\,(\phi_{kk}\,\delta_{mn} + \phi_{mn})\,d\phi_{mn} \qquad \text{.....(14)}$$

and elastic strain components for shear and normal part are given by:

$$d\epsilon_{ij}^{(e)} = \frac{1}{2G_s(\phi_{rs})}\,d\sigma_{ij} \qquad \text{for } i \neq j \qquad \text{.....(15)}$$

$$d\epsilon_{kk}^{(e)} = \frac{1}{3}\left[\frac{1}{3K_s(\phi_{rs})} - \frac{1}{2G_s(\phi_{rs})}\right]d\sigma_{kk} + \frac{1}{2G_s(\phi_{rs})}\,d\sigma_{jj} \quad \text{for } i = j$$

$$\text{.....(16)}$$

and volumetric strain

$$d\ell_{kk}^{(e)} = \frac{1}{3K_s(\phi_{rs})}\, d\sigma_{kk} \qquad \text{.....(17)}$$

The coefficient $A(\phi)$ and $B(\phi)$ are given by

$$A(\phi) = \frac{2K_o h}{(C_{ult})^2} \quad \text{and} \quad B(\phi) = \frac{nb\, G_o C\, (\phi_{ij})^{n-2}}{(C_{ult})^n} \qquad \text{.....(18)}$$

Here K_o and G_o are initial moduli and n, b and h are material constants. $C(\phi_{ij})$ is the intensity of crack tensor defined by

$$C(\phi_{ij}) = [(\phi_{kk})^2 + \phi_{ij}\,\phi_{ij}]^{1/2} \qquad \text{.....(19)}$$

and C_{ult} is the intensity of crack in uniaxial compression. K_s is the variable volumetric moduli and G_s is the variable shear moduli given by

$$K_s(\phi_{rs}) = K_o h \left(\frac{C(\phi_{k\ell})}{C_{ult}}\right)^2 \qquad \text{.....(20)}$$

$$G_s(\phi_{k\ell}) = G_o - \frac{b\, G_o\, (C(\phi_{ij}))^n}{(C_{ult})^m} \qquad \text{.....(21)}$$

The total strain component can be decomposed to purely elastic strain increment and fracturing strain increment as follows :

$$d\varepsilon_{ij} = d\varepsilon_{ij}^{(e)} + d\varepsilon_{ij}^{(f)} \qquad \text{.....(22)}$$

Stress Field for Region Containing Damaged Zone

In order to find the stress field in the region including the progressive of fracturing, the fracturing strain is used as a pseudo-body force to correct the stress field outside the damaged zone. The integral equations for the displacements and stress components including the accumulated fracturing strain increment are given in ref. 8

$$u_i(Q) = \int_{ABDC} U_i^{(q)}(Q,P)p_q^*(P)ds(P) + \int_A \Sigma_{ml}^{(i)}(Q,D)\,\varepsilon_{ml}^*(D)dA_D \quad \text{.....(23)}$$

and

$$\sigma_{ij}(Q) = \int_{ABDC} \Sigma_{ij}^{(q)}(Q,P)p_q^*(P)ds(P) + \int_A T_{ijml}(Q,D)\varepsilon_{ml}^*(D)dA_D - 2\mu\,\varepsilon_{ij}(Q)$$

..... (24)

where

$$T_{ijml} = \mu[\Sigma_{ml,j}^{(i)} + \Sigma_{ml,i}^{(j)} + \delta_{ij}\frac{2\nu}{1-2\nu}\Sigma_{ml,k}^{(k)}] \quad \text{.....(25)}$$

Here Q is the interior point, P is a point on the boundary ABDC, D is a point inside the damaged region A. p_q^* is again the fictitious traction component that has to be determined from the given boundary conditions. $\varepsilon_{ml}^*(D) = \varepsilon_{ml}^{(f)}(D)$ obtained from equation (12) is the accumulated fracturing strain components at the point D inside the region A. dA_D is the area element containing the point D. $\varepsilon_{ij}(Q) = \varepsilon_{ij}^{(e)}(Q)$ is obtained from equation (15). The boundary conditions to be satisfied are

$$(u_{i,j}+u_{j,i})n_j + \frac{2\nu}{1-2\nu}u_{k,k}n_i - 2\varepsilon_{ij}^*n_j = \frac{t_i}{\mu} \quad \text{.....(26)}$$

In order to solve for the vector $\vec{p}^*$, we let the point Q tend to P′ on the boundary ABDC and obtain

$$\frac{1}{2}p_i^*(P') + \int_{\substack{ABDC \\ P'\neq P}} \Sigma_{ij}^{(q)}(P',P)n_j(P')p_q^*(P)ds(P) + \int_A T_{ijml}(P',D)n_j(P')\,\varepsilon_{ml}^*(D)dA_D = t_i(P')$$

.....(27)

where the integrals are interpreted in the Cauchy Principal Value sense.

Note $\varepsilon_{ml}^*(P') = 0$ since the fracture has not yet reached the boundary.

Numerical Implementation

A general purpose computer program called BIEPEN (Boundary Integral Element Method for Penetration Problem) capable of solving planar brittle elastic problems including progressive fracturing has been written in FORTRAN language*. This program can be developed in 3-dimensional problem and use any other constitutive relation.

Boundary Integral Element for Plane Stress.

General analytic solutions to the integration of equations (6) and (27) are not available and it is, therefore, necessary to solve the equations numerically. The integral equations reduced to algebraic equations by discretizing the boundary into n straight line segments which are not necessarily equal. The center of each segment is called node P_l' or P_k' depending on whether the point is fixed or not with respect to the integration. The values of p_q^* and t_i are assumed to be constant on each segment and equal to the values calculated at the node.

Similarly, the interior of damaged region A is covered by a grid containing m cells which do not have to be equal in area. Their nodal points are located at the centroid D. The value of $\epsilon^*(D_e)$ is assumed to be constant over the e^{th} cell and equal to the value calculated at the centroid.

Under these conditions a discrete analog of the boundary integral equations (27) can be written as

$$\frac{1}{2} p_i^*(P_l') + \sum_{k=1}^{n} p_q^*(P_k)\, \Delta I_{iq}(P_l', P_k) + \sum_{e=1}^{m} \epsilon_{ml}^*(D_e)\, \Delta J_{iml}(P_l', D_e) = t_i(P_l') \quad , \qquad \text{.....(28)}$$

where

$$\Delta I_{iq}(P_l', P_k) = \int_{s_k}^{s_{k+1}} \Sigma_{ij}^{(q)}(P_l', P_k) n_j(P_l') ds(P_k) \qquad \text{.....(29)}$$

$$\Delta J_{iml}(P_l', D_e) = \int_{\Delta A_e} T_{ijml}(P_l', D_e)\, n_j(P_l')\, dA_e \qquad \text{.....(30)}$$

---

* The problem in this paper was run on a CDC 6500

Details of these calculations are available in ref. 8. Equation (28) can be expressed in matrix form

$$\{\frac{1}{2}\,[I] + [\Delta I]\}\,\{p^*\} = \{t\} - \{\varepsilon^*\,\Delta J\} \qquad \text{.....(31)}$$

where $[I]$ is the identity matrix. Equation (31) has been solved by a standard Gauss reduction scheme on $\left\{\frac{1}{2}\,[I] + [\Delta I]\right\}$ followed by an iteration to refine the solution $\{p^*\}$.

Finally, after solving equation (31), the now completely known fictitious boundary data may be used to determine the solution for the internal stresses from equation (24) which can be written as,

$$\sigma_{ij}(Q) = \sum_{k=1}^{n} p_q^*(P_k)\;\Delta K_{ijq}(Q,P_k) + \sum_{e=1}^{m} \varepsilon_{ml}^*(D_e)\,\Delta M_{ijml}(Q,D_e) - 2\mu\varepsilon_{ij}(Q) \qquad \text{.....(32)}$$

The integrations to determine ΔK and ΔM are given by :

$$\Delta K_{ijq}(Q,P_k) = \int_{s_k}^{s_{k+1}} \Sigma_{ij}^{(q)}(Q,P_k)\; ds(P_k) \qquad \text{.....(33)}$$

$$\Delta M_{ijml}(Q, D_e) = \int_{\Delta A_e} T_{ijml}(Q, D_e)\; dA_e \qquad \text{.....(34)}$$

Any number of interior solutions may be made when the boundary solution is obtained. Since the solution is performed at pre-selected points, an analyst may concentrate on any particular area of interest and is not burdened with complete field solutions.

Note that in order to find the internal stresses before the incipient of the fracture, the numerical unknown value p_q^* from equation (6) can be calculated from equation (28) by letting $\varepsilon_{ml}^* = 0$. Then the known p_q^* may again be used to determine the solution for the internal stresses from equation (3). The numerical result of equation (3) can be obtained from equation (32) by letting both ε_{ml}^* and ε_{ij} be equal to zero.

Results and Discussion

The region considered is $R = \{(x, y)/.15 \leq x \leq 1.0, -1.0 \leq y \leq -.15\}$ which is located interior to the rock mass at a distance approximately $\frac{1}{8}$ of the slant from the boundary. There are 246 points altogether as shown in Figure 4. The points are numbered consecutively from the coordinates (.15, - .75), (.15, - .80) ... and so on. The interior of damaged region A is covered by square grids each of size .025 × .025 sq.in. In order to divide the boundary ABDC or DBAC, we have to consider each portion separately. Since the traction distributes only along the portion AB, and there is no traction along the portion BD and AC, so we have to divide the portion AB and that near AB very precisely as follows.

Let the length of the boundary DBAC be 5 inches where the portions DB = 2, BA = 1, and AC = 2 inches respectively. The portion BA is divided to 32 equal parts each of length $\frac{1}{32}$ inch while the portion BD is divided to 4 equal parts. The first two parts from the end point D is subdivided to 8 parts each of length $\frac{1}{8}$ inch. The third part of DB is subdivided to 8 parts each of length $\frac{1}{16}$ and the last portion near BA is subdivided to 16 parts each of length $\frac{1}{32}$ inch. The portion AC is divided in the same manner as DB (see Figure 2). There are altogether 96 discretized boundary data elements.

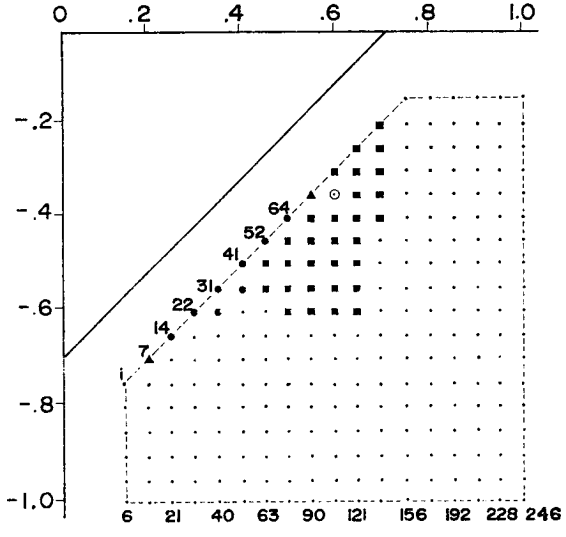

Figure 4 Region (R) with specified 246 interior points is considered. As the load has been increased up to 1.24% of the critical load, cracks initiate at point (●) for 1st iteration and points (▲), (⊙) and (■) are consequently brought into the damaged region for 2nd, 3rd, and 4th iterations respectively.

The value of the parameters used and the material constants are F = 1 lb/in.^{2}, L = 1 in., m = 5, $\theta = \pi/4$, $\phi_f = 0$, n = 1, b = 1, h = 1, E = 6371 ksi, $\nu = .34$, S_t = 1.3 ksi, S_c^i = 8.8 ksi, S_c = 17.6 ksi. From the calculations, the critical load obtained from the minimum of K^i = 3.215 lb/in^2 is located at the position 52. At this point there is the possibility for a crack to develop and initiate. When the load has been increased about 0.62% from the critical load i.e., F = 3.235 lb/in^2 it is found that there are five points at the positions, 22, 31, 41, 52 and 64 outside the elastic surface. Consequently, these points meet the criteria for crack initiation. The fracturing strain increments from these five points have been calculated by assuming a linear stress increment for the first iteration. Then, the calculated fracturing strain will be used as a pseudo-body force for calculating the stress field for the second iteration. It is found that there is one more point at the position 14 that slips into the damaged region. After the third iteration has been carried out by taking the effect of the new point into account, it is found that there are no more points brought into the damaged region. This means that when the load is increased 0.62% from the critical load, the fracture propagation becomes stable. The principal stresses for the points that are far away from the damaged region give a better convergence than those that are close to the damaged region (see Table 1 and Table 2). The percentage of the stress convergence is no worse than 99.68% for the points that are close to the damaged region and about 99.96% for the points that far away from the damaged region.

For the load increases 1.08% of the critical load, there are seven points in the damaged region which locate at the positions 14, 22, 31, 32, 41, 52 and 64. For the second iteration, there is one more point at the position 7 brought into the damaged region. The third iteration has been carried out by taking the effect of the new point into account. It is found that there are no more points brought into the damaged region. The fracture propagation is still stable and the growing damaged region becomes shallow and longer in the horizontal direction. The principal stresses for the points that are far away and close to the damaged region are given in Table 3 and Table 4. The percentage of the stress convergence is no worse than 99.65% and 99.92% for the points that are close and far away from the damaged region.

For the load increases 1.24% of the critical load, there are eight points in the damaged region at the positions 14, 22, 31, 32, 41, 42, 52, and 64 as shown in Figure 4. These have been calculated by using the first iteration. For the second iteration, there are two more points brought into the damaged region at the positions 7 and 77. For the third iteration, after taking these two new points into account and recalculating stresses again, it is found that there is one more point at the position 92 brought into the damaged region. This point has very low crack intensity, so it gives very large fracturing strain increment and this will give a large effect when this point is considered as a new pseudo-body force for the fourth iteration. After the fourth iteration has been carried out, it is found that

TABLE 1 Comparison between principal stresses at load (P/L = 3.235) increment 0.62% from the critical load (P/L = 3.215) by assuming linearity for the 1st iteration and after taking the effect of fracturing strain for the 2nd and 3rd iteration for the points that are close to the damage region.

Location	1 st iteration		2 nd iteration		% change 1st vs 2nd		3rd iteration		% change 1st vs 3rd		% change 2nd vs 3rd	
	σ_1	σ_2	σ_1	σ_2	σ_1	σ_2	σ_1	σ_2	σ_1	σ_2	σ_1	σ_2
16	.157662	-7.407252	.159458	-7.408964	-1.1	-.02	.159041	-7.408580	-.87	-.01	.26	.01
25	.258932	-6.985652	.256636	-6.982656	.89	.04	.255827	-6.981849	1.2	.05	.32	.01
35	.356011	-6.485186	.350040	-6.478202	1.7	.11	.349467	-6.477608	1.8	.12	.16	.01
46	.437073	-5.964617	.430545	-5.956927	1.5	.13	.430198	-5.956591	1.6	.13	.08	.01
58	.497843	-5.458607	.492467	-5.452143	1.1	.11	.492247	-5.451884	1.1	.12	.04	.00
71	.538685	-4.985708	.534677	-4.980722	.74	.10	.534527	-4.980533	.77	.10	.03	.00
85	.562275	4.554265	.559393	-4.550549	.51	.08	.559283	-4.550402	.53	.08	.02	.00
93	1.088743	-2.847192	1.097774	-2.857216	-.83	-.35	1.097740	-2.857149	-.83	-.35	.00	.00
94	1.022610	-3.300964	1.028175	-3.306860	-54	-.18	1.028135	-3.306778	-54	-.18	.00	.00
85	.945633	-3.670717	.947036	-3.671932	-15	-.03	.946587	-3.671836	-10	-.03	.05	.00
96	.864544	-3.944633	.863669	-3.943232	.10	.04	.863610	-3.943123	.11	.04	.01	.00
97	.784302	-4.121607	.782342	-4.118941	.23	.06	.782271	-4.118822	.23	.00	.01	.00
98	.707956	-4.208800	.705619	-4.205699	.33	.07	.705539	-4.205575	.34	.08	.01	.00
99	.637037	-4.218731	.634737	-4.215686	.36	.07	.634653	-4.215562	.37	.08	.01	.00
100	.572101	-4.166486	.570055	-4.163734	.36	.07	.569971	-4.163617	.37	.07	.01	.00

TABLE 2 Comparison between principal stresses at load (P/L = 3.235) increment 0.62% from the critical load (P/L = 3.215) by assuming linearity for the 1st iteration and after taking the effect of fracturing strain for the 2nd and 3rd iteration for the points that are far away from the damage region.

Location	1 st iteration		2 nd iteration		% change 1st vs 2nd		3rd iteration		% change 1st vs 3rd		% change 2nd vs 3rd	
	σ_1	σ_2	σ_1	σ_2	σ_1	σ_2	σ_1	σ_2	σ_1	σ_2	σ_1	σ_2
21	.125653	-4.198054	.125135	-4.197534	.41	.10	.125082	-4.197502	.45	.01	.04	.00
40	1.98781	-4.146515	.198014	-4.145536	.39	.02	.197949	-4.145476	.42	.03	.03	.00
63	.264196	-3.924655	.263344	-3.923459	.32	.03	.263284	-3.923392	.34	.03	.02	.00
90	.314215	-3.616069	.313445	-3.614916	.24	.03	.313397	-3.614854	.26	.03	.02	.00
121	.346661	-3.282227	.346048	-3.281251	.18	.03	.346011	-3.281197	.19	.03	.01	.00
35	.363488	-2.959049	.363028	-2.958273	.13	.03	.362999	-2.958227	.13	.03	.01	.00
71	.368422	-2.663651	.368084	-2.663049	.09	.02	.368061	-2.663010	.10	.02	.01	.00
108	.557416	-1.040878	.557587	-1.041232	-.03	-.03	.557565	-1.041213	-.03	-.03	.00	.00
110	.561784	-1.282592	.561963	-1.282986	-.03	-.03	.561940	-1.282961	-.03	-.03	.00	.00
112	.565536	-1.552050	.565673	-1.552375	-.02	-.02	.565649	-1.552345	.61	-.02	.00	.00
114	.557925	-1.811496	.557973	-1.811660	-.01	-.01	.557948	-1.811625	.00	.00	.00	.00
116	.536628	-2.030981	.536565	-2.030940	.01	.00	.536540	-2.030902	.02	.00	.00	.00
118	.504148	-2.191953	.503988	-2.091728	.03	.01	.503963	-2.191689	.04	.01	.00	.00
120	.464792	-2.288062	.464573	-2.287713	.05	.02	.464550	-2.287674	.05	.02	.00	.00
112	.422782	-2.323030	.422544	-2.322621	.06	.02	.422523	-2.322585	.06	.02	.00	.00
125	.361647	-2.283482	.361433	-2.283069	.06	.02	.361416	-2.283037	.06	.02	.00	.00

TABLE 3 Comparison between principal stresses at load (P/L = 3.250) increment 1.08% from the critical load (P/L = 3.215) by assuming linearity for the 1st iteration and after taking the effect of fracturing strain for the 2nd and 3rd iteration for the points that are far away from the damage region.

Location	1 st iteration		2 nd iteration		% change 1st vs 2nd		3rd iteration		% change 1st vs 3rd		% change 2nd vs 3rd	
	σ_1	σ_2	σ_1	σ_2	σ_1	σ_2	σ_1	σ_2	σ_1	σ_2	σ_1	σ_2
21	.126236	-4.217520	.123698	-4.214099	2.01	.08	.123596	-4.214083	2.09	.08	.08	.00
40	.199703	-4.165742	.196375	-4.160964	1.67	.11	.196307	-4.161014	1.70	.11	.03	.00
63	.265422	-3.942853	.262124	-3.937856	1.24	.13	.262081	-3.937908	1.26	.13	.02	.00
90	.315672	-3.632836	.312932	-3.728451	.87	.12	.312902	-3.628482	.88	.12	.01	.00
121	.348268	-3.297446	.346208	-3.293961	.59	.11	.346186	-3.293976	.60	.11	.01	.00
35	.365172	-2.972770	.363699	-2.970136	.40	.09	.363682	-2.970140	.41	.09	.00	.00
71	.370130	-2.676002	.369097	-2.674050	.28	.07	.369084	-2.674050	.28	.07	.00	.00
108	.560000	-2.045705	.561120	-1.047663	-.20	-.19	.561111	-1.047647	-.20	-.19	.00	.00
110	.564398	-1.288539	.565574	-1.290803	-.21	-.18	.565567	-1.290782	-.21	-.17	.00	.00
112	.568158	-1.559247	.569206	-1.561347	-.18	-.13	.569127	-1.561322	-.18	-.13	.00	.00
114	.560512	-1.819897	.561213	-1.821410	-.13	-.08	.561198	-1.821383	-.12	-.08	.00	.00
116	.539116	-2.040399	.539362	-2.041097	-.05	-.03	.539346	-2.041069	-.04	-.03	.00	.00
118	.506486	-2.202117	.506311	-2.202024	.03	.00	.506295	-2.202000	.04	.00	.00	.00
120	.466947	-2.298671	.466485	-2.297982	.10	.03	.466470	-2.297963	.10	.03	.00	.00
122	.424742	-2.333801	.424143	-2.332749	.14	.05	.424130	-2.332737	.14	.05	.00	.00
125	.363324	-2.294070	.362721	-2.292814	.17	.05	.362711	-2.292809	.17	.05	.00	.00

TABLE 4 Comparison between principal stresses at load (P/L = 3.250) increment 1.08% from the critical load (P/L = 3.215) by assuming linearity for the 1st iteration and after taking the effect of fracturing strain for the 2nd and 3rd iteration for the points that are close to the damage region.

Location	1 st iteration		2 nd iteration		% change 1st vs 2nd		3rd iteration		% change 1st vs 3rd		% change 2nd vs 3rd	
	σ_1	σ_2	σ_1	σ_2	σ_1	σ_2	σ_1	σ_2	σ_1	σ_2	σ_1	σ_2
16	.158394	-7.441548	.147098	-7.427714	7.13	.19	.145634	-7.429050	8.05	.17	.10	.02
25	.260133	-7.018043	.230027	-6.983931	11.57	.49	.229215	-6.984016	11.88	.48	.35	.00
35	.357662	-6.515257	.328255	-6.481194	8.22	.52	.327808	-6.481077	8.35	.52	.14	.00
46	.439099	-5.992274	.415809	-5.964347	5.30	.47	.415540	-5.964220	5.37	.47	.06	.00
58	.500152	-5.483918	.483003	-5.462579	3.43	.39	.482827	-5.462470	3.46	.39	.04	.00
71	.541182	-5.008827	.528860	-4.992960	2.28	.32	.528738	-4.992871	2.30	.32	.02	.00
85	.564882	-4.575382	.556135	-4.563779	1.55	.25	.556046	-4.563705	1.56	.26	.02	.00
93	1.093791	-2.860294	1.132560	-2.904671	-3.54	-1.55	1.132558	-2.904597	-3.54	-1.55	.00	.00
94	1.027352	-3.316270	1.050237	-3.342224	-2.24	-.78	1.050327	-3.324137	-2.24	-.78	.00	.00
95	.950018	-3.687737	.956030	-3.694625	-.63	-.19	.956008	-3.694523	-.63	-.18	.00	.00
96	.868553	-3.362942	.866666	-3.960411	.22	.06	.866632	-3.960300	.22	.07	.00	.00
97	.787939	-4.140718	.782662	-4.133875	.70	.17	.782613	-4.133762	.68	.10	.01	.00
98	.711239	-4.228316	.704716	-4.219736	.92	.20	.704655	-4.219631	.93	.21	.01	.00
99	.639990	-4.238293	.633349	-4.229415	1.04	.21	.633282	-4.229329	1.05	.21	.01	.00
100	.574753	-4.185787	.568606	-4.177415	1.07	.20	.568539	-4.177354	1.08	.20	.01	.00

TABLE 5 Comparison between principal stresses at load (P/L = 3.255) increment 1.24% from the critical load (P/L = 3.215) by assuming linearity for the 1st iteration and after taking the effect of fracturing strain for the 2nd and 3rd iteration for the points that are close to the damage region

Location	1 st iteration		2 nd iteration		% change 1st vs 2nd		3rd iteration		% change 1st vs 3rd		% change 2nd vs 3rd	
	σ_1	σ_2	σ_1	σ_2	σ_1	σ_2	σ_1	σ_2	σ_1	σ_2	σ_1	σ_2
16	.158637	-7.453047	.144234	-7.426906	9.08	.35	.139256	-7.419093	12.21	.46	3.45	.11
25	.260533	-7.028840	217717	-6.980389	16.43	.69	.215113	-6.977837	17.43	.73	1.20	.04
35	.358212	-6.525280	.317743	-6.486263	11.3	.60	.315775	-6.483883	11.84	.63	.62	.04
46	.439775	-6.001439	.410755	-5.975507	6.60	.43	.408478	-5.9272107	7.62	.49	.55	.06
58	.500922	-5.492350	.480848	-5.473983	4.00	.33	.478333	-5.470110	4.51	.40	.52	.07
71	.542015	-5.016530	.527957	-5.002847	2.59	.27	.525385	-4.998979	3.07	.35	.49	.08
85	.565751	-4.582430	.555927	-4.572277	1.74	.22	.553487	-4.568741	2.17	.30	.44	.08
93	1.095474	-2.864794	1.149742	-2.924064	-4.95	-2.07	1.135179	-2.912374	-3.62	-2.66	1.27	.40
94	1.028932	-3.321371	1.061200	-3.355326	-3.14	-1.02	1.037014	-3.332331	-.79	-.33	2.88	.69
95	.951479	-3.693410	.960301	-3.701556	-.93	-.22	.945281	-3.686676	.65	.18	1.56	.40
96	.869888	-3.969021	.867998	-3.965305	.22	.09	.858555	-3.955395	1.30	.34	1.09	.25
97	.789151	-4.147088	.782919	-4.138931	.79	.20	.776679	-4.131920	1.59	.37	.80	.17
98	.712332	-4.234821	.704776	-4.225812	1.06	.21	.700493	-4.220646	1.66	.33	.61	.12
99	.640975	-4.244813	.633514	-4.236451	1.16	.20	.630505	-4.232553	1.63	.29	.47	.09
100	.575637	-4.192227	.568871	-4.184916	1.17	.17	.566729	-4.181924	1.55	.25	.38	.07

there are quite a few points near the damaged region which move into the damaged region. This means that the damaged region starts growing very rapidly and becomes larger and larger. The shape of the growing region is observed to grow in both horizontal and vertical directions. Finally, this region has a great effect on the stress field in the undamaged region as follows. The stress at points along a specified vertical line in the elastic region remains in a tension-compression state, and is consequently more likely to fracture, whereas the stress at points along a specified horizontal line changes from the state of tension-compression to compression-compression. Therefore, it is less likely to fracture. The stresses become divergent as shown in Table 5. The fracture propagation is now an unstable propagation. Thus, it can be concluded that the calculated stress is accurate up to the load increment less than 1.24% of the critical load.

The stress path for a particular point such as at the position 93 is concave upward from the straight line before it passes outside the elastic surface as shown in Figure 3. This is the result from the stress correction for every loading increment from 3.215 lb/in^2 to 3.255 lb/in^2.

Conclusion

It has been clearly demonstrated that the Boundary Integral Element method provides a very useful technique for carrying out the analysis of the penetration problem. The method can also apply for any failure criteria of the material and other constitutive laws for fracturing strain. It can be extended to the solution of problems concerning drilling in 3-dimensional solids such as those found in geotechnical engineering.

Acknowledgements

The author would like to express her appreciation to Prof. Z. Mroz for his valuable suggestion and reading this manuscript.

References

1. Mendelson, A. (1973) *Boundary-Integral Methods in Elasticity and Plasticity,* NASA TND 7418.
2. Mendelson, A. and Alber, L.U. (1975) Application of Boundary Integral Equations to Elastoplastic Problems. *Boundary - Integral Equation Method : Computational Applications in Applied Mechanics,* Cruse, T.A., and Rizzo, F.J., eds., ASME 47-84.
3. Rizzo, F.J. (1967) An Integral Equation Approach to Boundary Value Problems of Classical Elastostatics. *Quart. Appl. Math.* **25**, 83-95.
4. Cruse, T.A. (1969) Numerical Solutions in Three Dimensional Elastostatics. *Int. J. Solids and Struct.* **5**, 1259-1274.
5. Swedlow, J.L. and Cruse, T.A. (1971) Formulation of the Boundary Integral Equations for Three-dimensional elastoplastic Flow. *Int. J. Solids and Struct.* **7**, 1673-1681.
6. Cruse, T.A. and Rizzo, F.J. (1975) *Boundary Integral Equation Method: Computational Applications in Applied Mechanics,* ASME AMD. 11, New York.

7. Sikarski, D.L. and Altiero, N.J. (1973) The Formation of Chips in the Penetration of Elastic-Brittle Materials (Rock). *Jour. of Applied Mechanics* **40**, 791-798.
8. Wasuwanich, S. (1986) Response of Brittle Elastic Material: Boundary Integral Element Approach. *The Kasetsart Journal (Scince)* **20**, 50-57.
9. Sadeah, A. (1978) *On the Problem of a Plane, Finite Linear-Elastic Region Containing a Hole of Arbitrary Shape, A Boundary Integral Approach,* Ph.D. Thesis, Michigan State University.
10. Altiero, N.J. and Sikarski, D.L. (1975) An Integral Equation Method Applied to Penetration Problems in Rock Mechanics: *Boundary Integral Equation Method, Computational Applications in Applied Mechanics,* AMD. 11 ASME 119-141.
11. Vile, G. W.D. (1968) The Strength of Concrete Under Short-term Static Biaxial Stress. *The Structure of Concrete, Cem. Concrete Ass.,* ed. A.E. Brooks, K. Newman 275-288.
12. Altiero, N.J. (1976) On the Edge-Fracture of Rock Mechanics. *Mech. Res. Com.* **3**, 354-362.
13. Dragon, A. (1976) On Phenomenological Description of Rock-like Materials with Account for Kinetics of Brittle Fracture. *Archives of Mechanics* **28**, 13-30.
14. Dragon, A. and Mroz, Z. (1979) A Continuum Model for Plastic-Brittle Behavior of Rock and Concrete. *Int. J. Engng. Sci.* **17**, 121-137.

บทคัดย่อ

ในบทวิจัยที่จะกล่าวถึงนี้ เป็นการศึกษาการก่อตัวของสะเก็ดวัตถุที่ได้จากการเจาะวัตถุที่มีความยืดหยุ่นและเปราะ เช่น หิน โดยเครื่องมือเจาะมีลักษณะเป็นลิ่มทำด้วยวัสดุแข็ง

โดยอาศัยการคำนวณเชิงตัวเลขของการวิเคราะห์สนามความเค้นโดยสมการบาวดารี อินทิกรัล จากบทวิจัยที่ผ่านมา พบว่าตำแหน่งที่รอยร้าวเริ่มก่อตัวอยู่ในแนวเส้นตั้งฉากที่ลากจากจุดกึ่งกลางของขอบบนลิ่มกับด้านข้างของลิ่ม เมื่อแรงกดเพิ่มขึ้นน้อยกว่า 1.24% จากแรงวิกฤติ รอยร้าวจะเริ่มแผ่กระจาย ทำให้บริเวณส่วนบุบสลายขยายตัวไปรอบลิ่ม ส่วนบุบสลายนี้มีลักษณะตื้นและค่อย ๆ ยาวขึ้นในทิศขนานกับขอบลิ่มและจะแผ่ออกไปทั้งในทิศแนวราบและแนวดิ่ง stress ที่จุดใกล้ ๆ บริเวณบุบสลายจะมีผลต่อการถูกกระทบมากกว่าจุดที่ไกลออกไป ทางเดินของ stress บางจุดจะเปลี่ยนจากเส้นตรงเป็นเส้นโค้งมีลักษณะเว้าขึ้น ถ้าแรงกดเพิ่มขึ้นเกิน 1.24% ของแรงวิกฤติรอยร้าวไม่สามารถควบคุมได้